

Nuclear Inst. and Methods in Physics Research, A

Development of Multi-element Monolithic Germanium Detectors for X-ray Detection at Synchrotron Facilities

--Manuscript Draft--

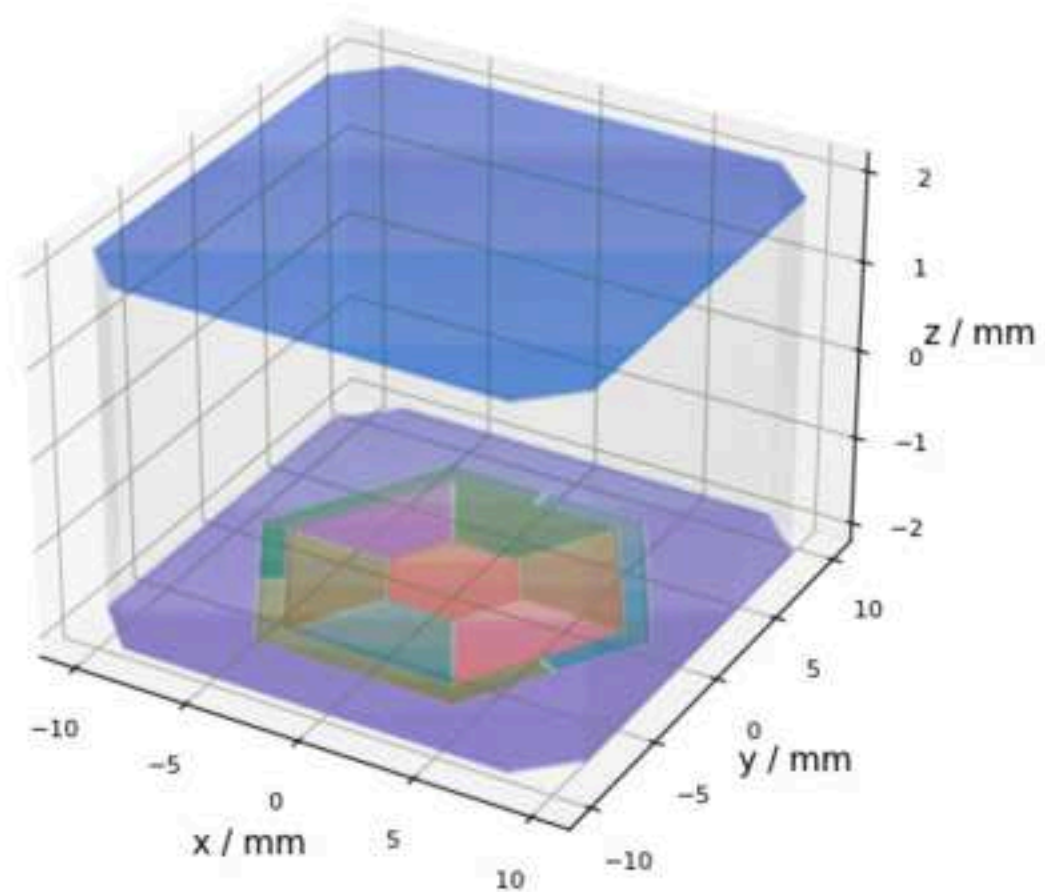
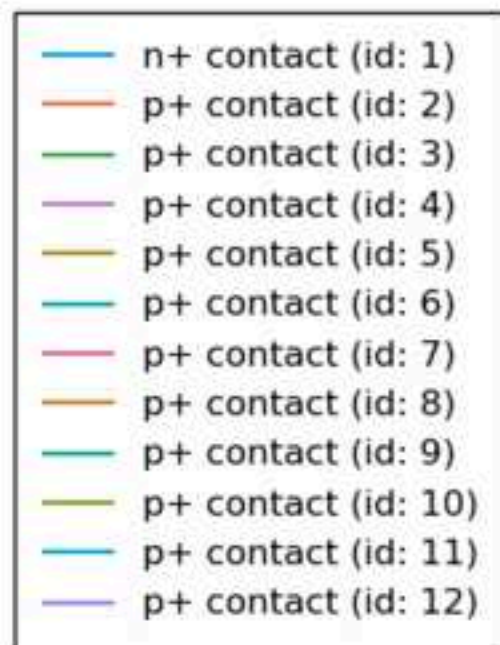
Manuscript Number:	
Article Type:	VSI: NDIP20
Keywords:	Germanium detectors Semiconductors Synchrotrons
Corresponding Author:	Luis Manzanillas Velez, Ph.D. SOLEIL Gif-sur-Yvette, FRANCE
First Author:	Luis Manzanillas Velez, Ph.D.
Order of Authors:	Luis Manzanillas Velez, Ph.D. Fabienne Orsini Francisco Jose Iguaz Nicola Tartoni Graham Dennis Sudeep Chatterji Heinz Graafsma Edmund Welter Helmut Hirsemann Joan Casas Marcos Quispe Ralf Menk Pablo Fajardo Cédric Cohen Thierry Martin Steve Alpin Matteo Porro Monica Turcato Antonella Balerna Paul Bell Michele Cascella Chris Ward Konstantin Klementiev Bernd Schmitt Tomasz Kołodziej
Abstract:	In past years efforts have concentrated to the developments of arrays of Silicon Drift Detectors for X-ray spectroscopy. This is in stark contrast to the little effort that has been devoted to the improvement of germanium detectors, in particular for synchrotron applications. Germanium detectors enable to detect with better energy resolution and more efficiently photons of considerable higher energy with respect to silicon detectors.

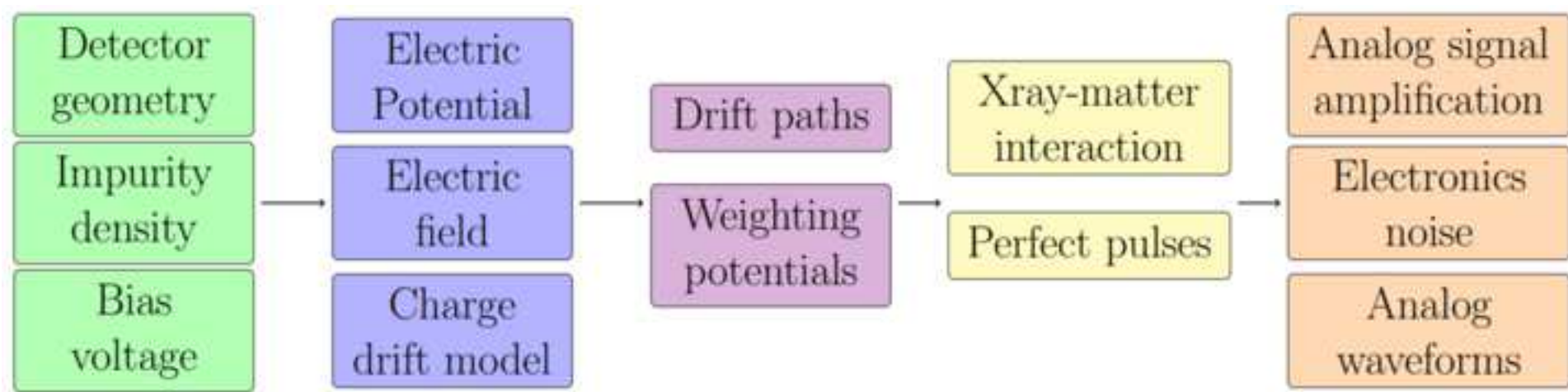
In this context, the detector consortium of the European project LEAPS-INNOV has set an ambitious R&D program devoted to the development of a new generation of multi-element monolithic germanium detectors for X-ray detection. In order to improve the performance of the detector under development, physics simulations of the different detector design options have been performed. In this contribution, the efforts in terms of R&D are outlined with focus on the modelization of the detector geometry and first performance results.

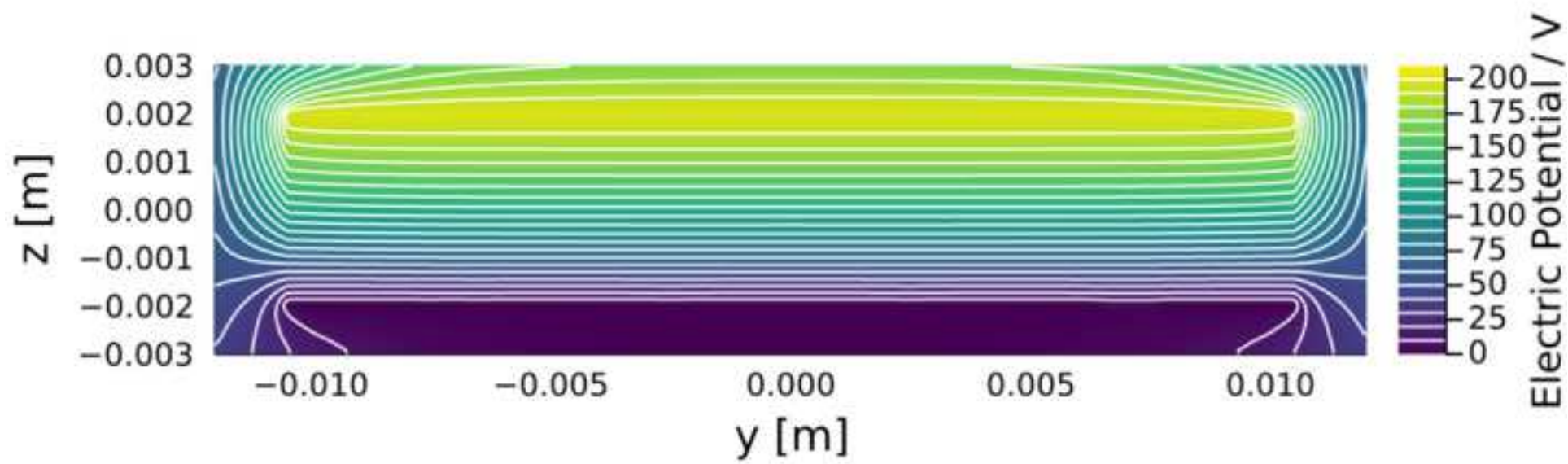


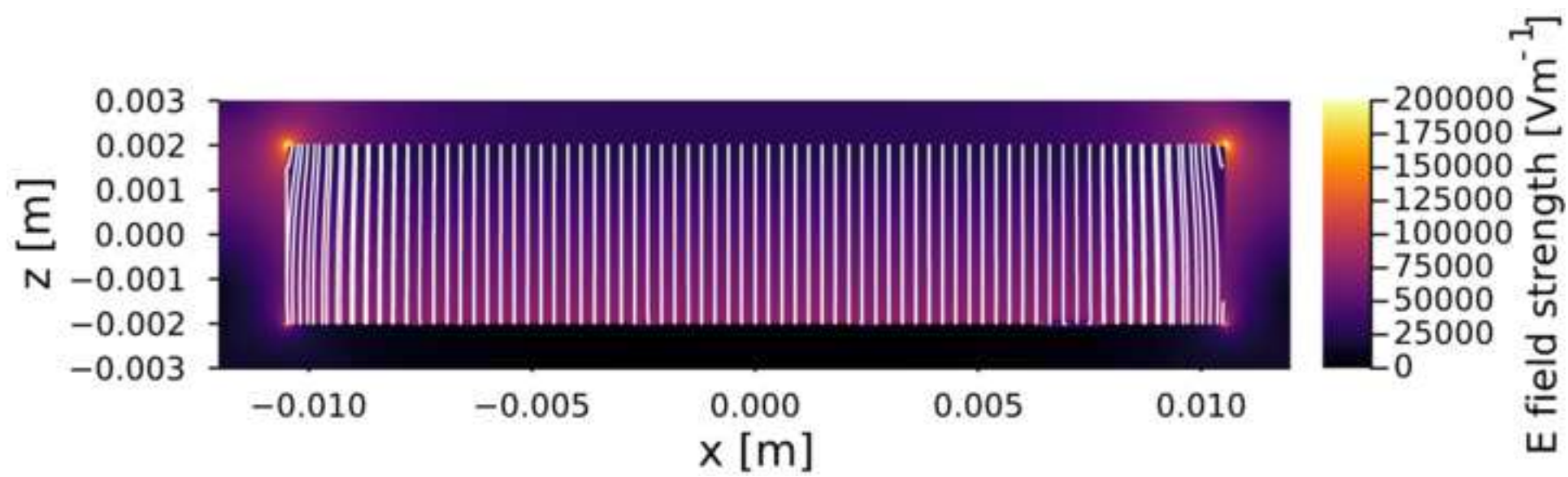
Click here to access/download
LaTeX Source Files
ndip_manzanillas.tex

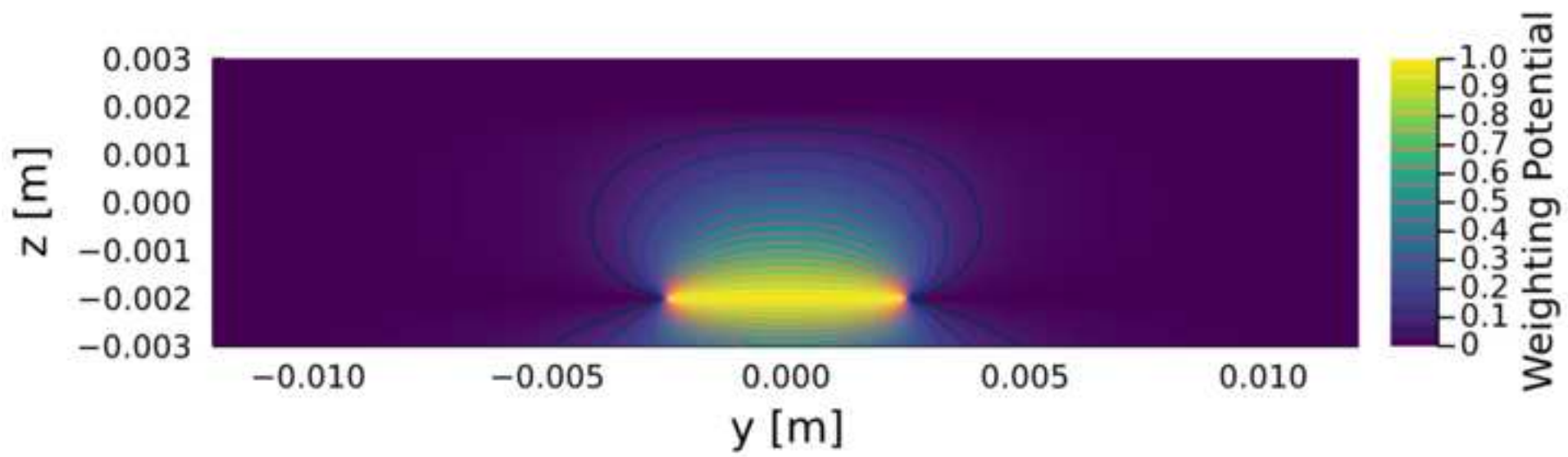






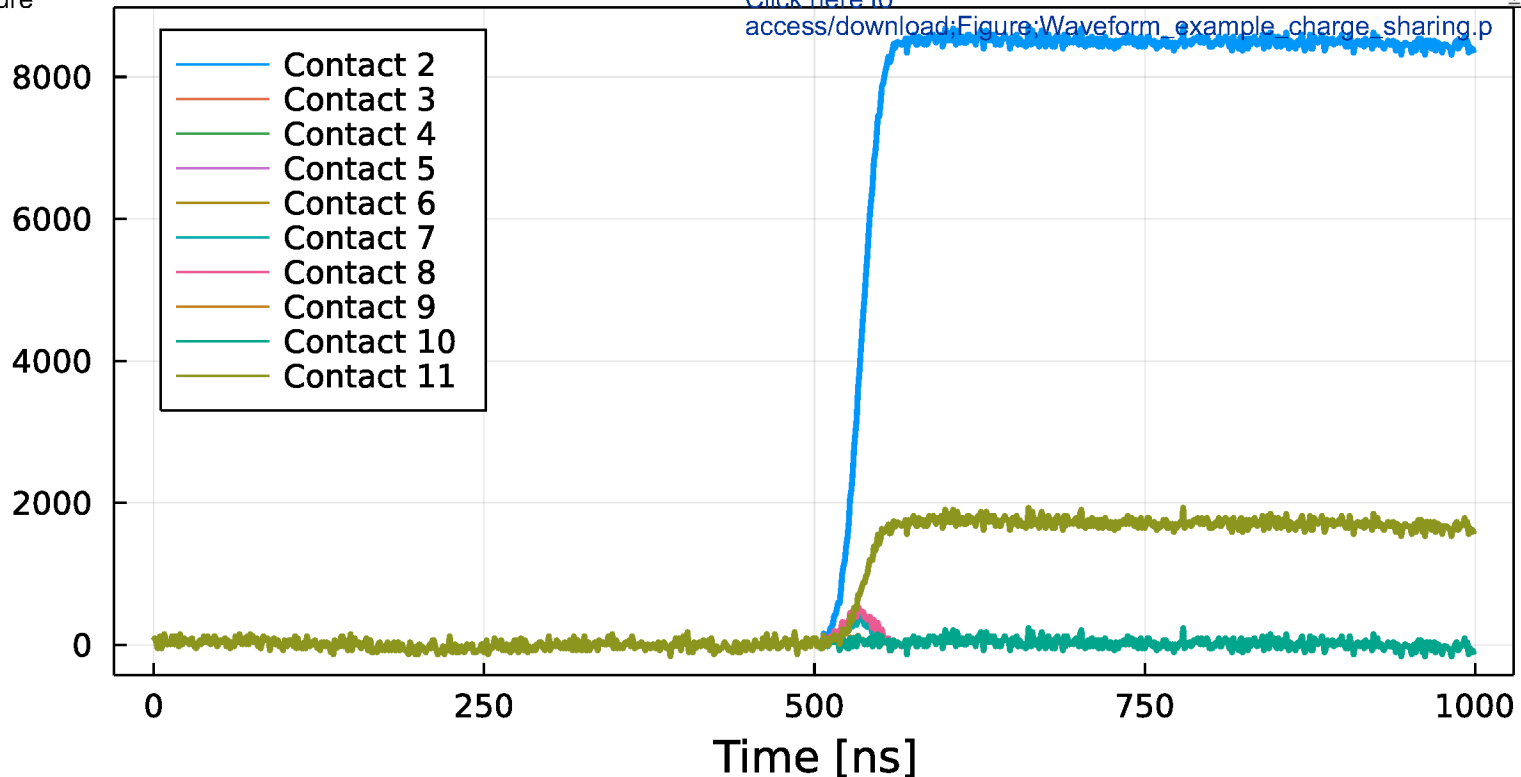






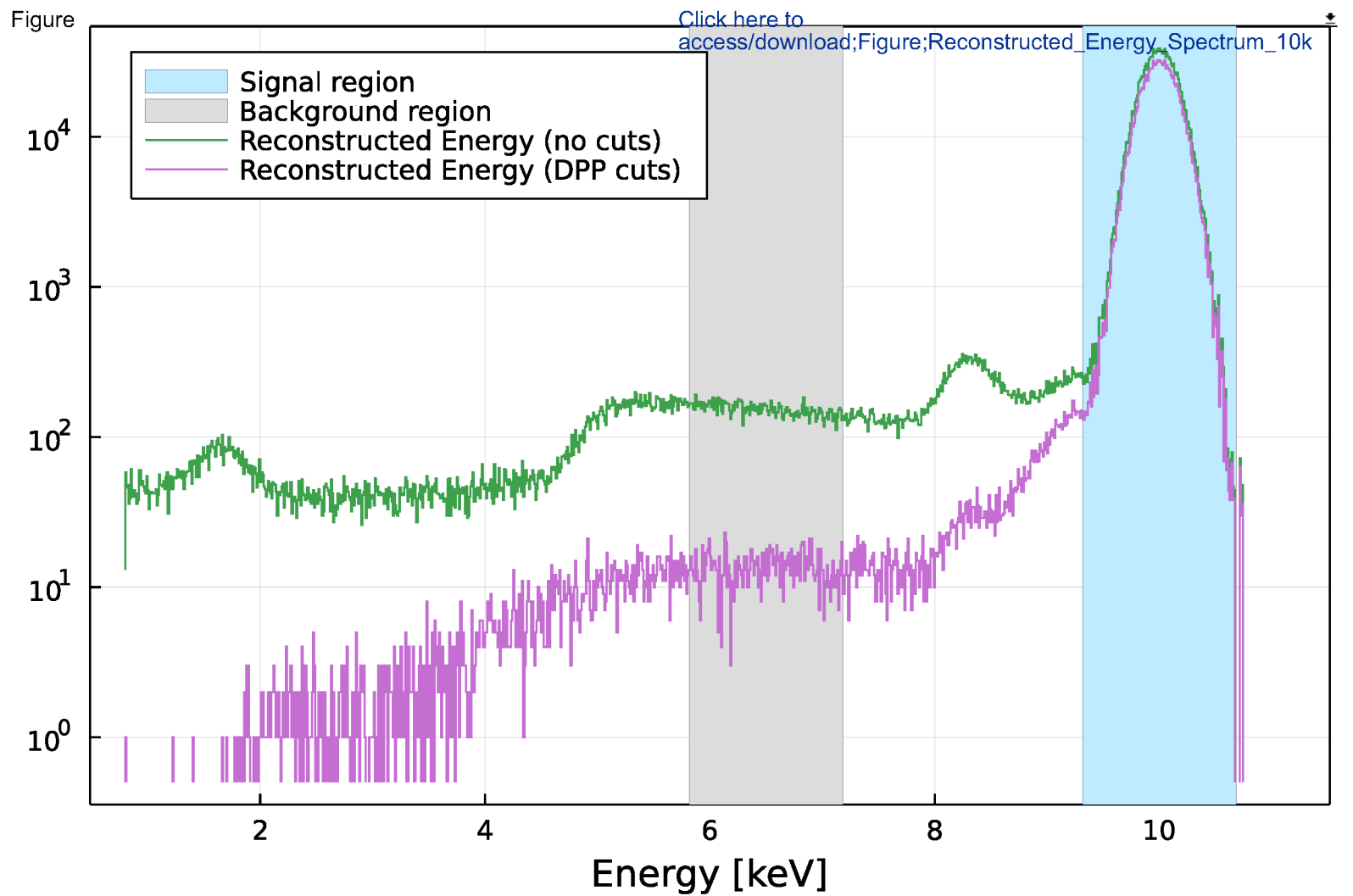
Figure

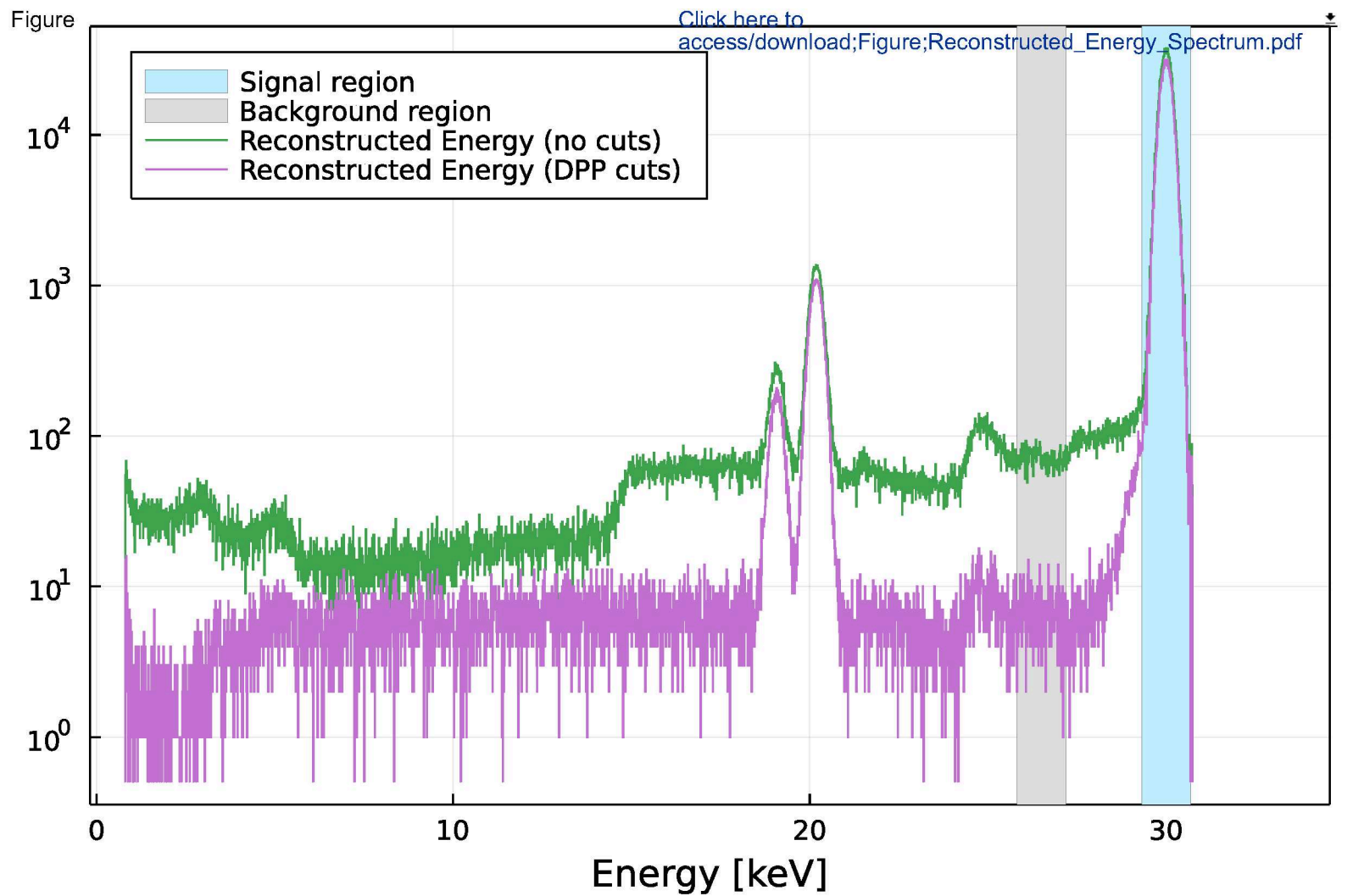
sample value [e]

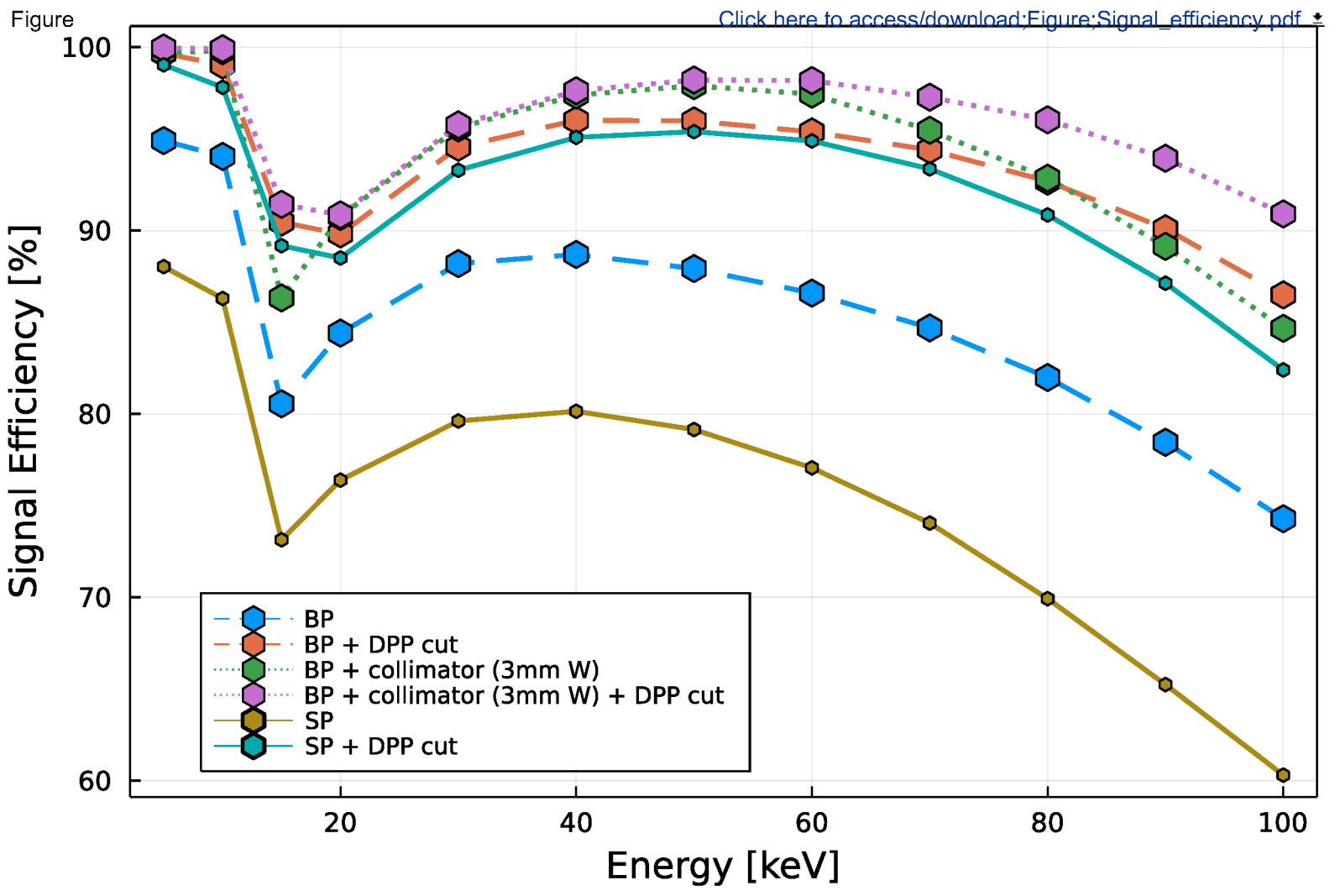


[Click here to access/download:Figure:Waveform_example_charge_sharing.p](#)

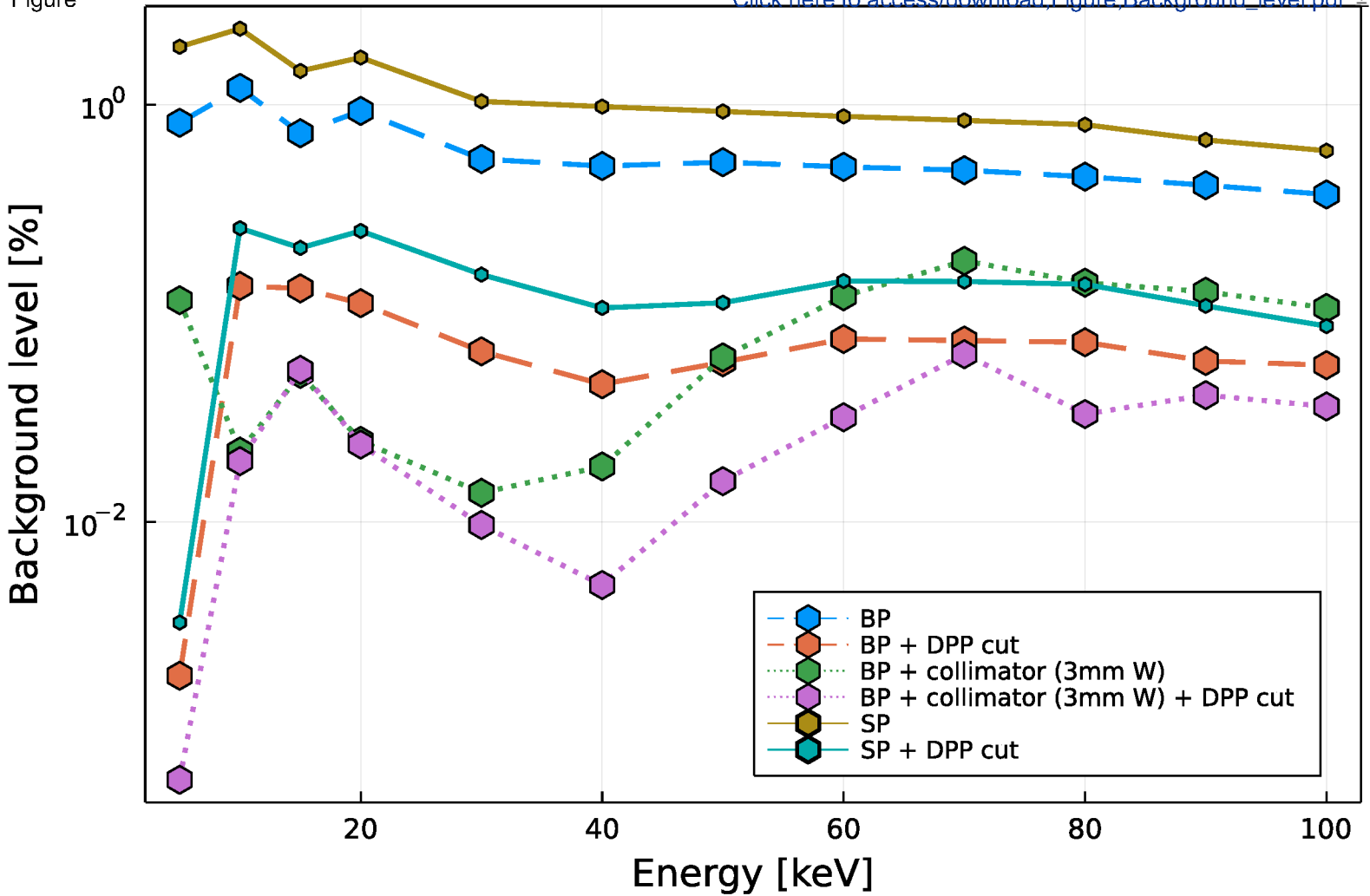
Time [ns]

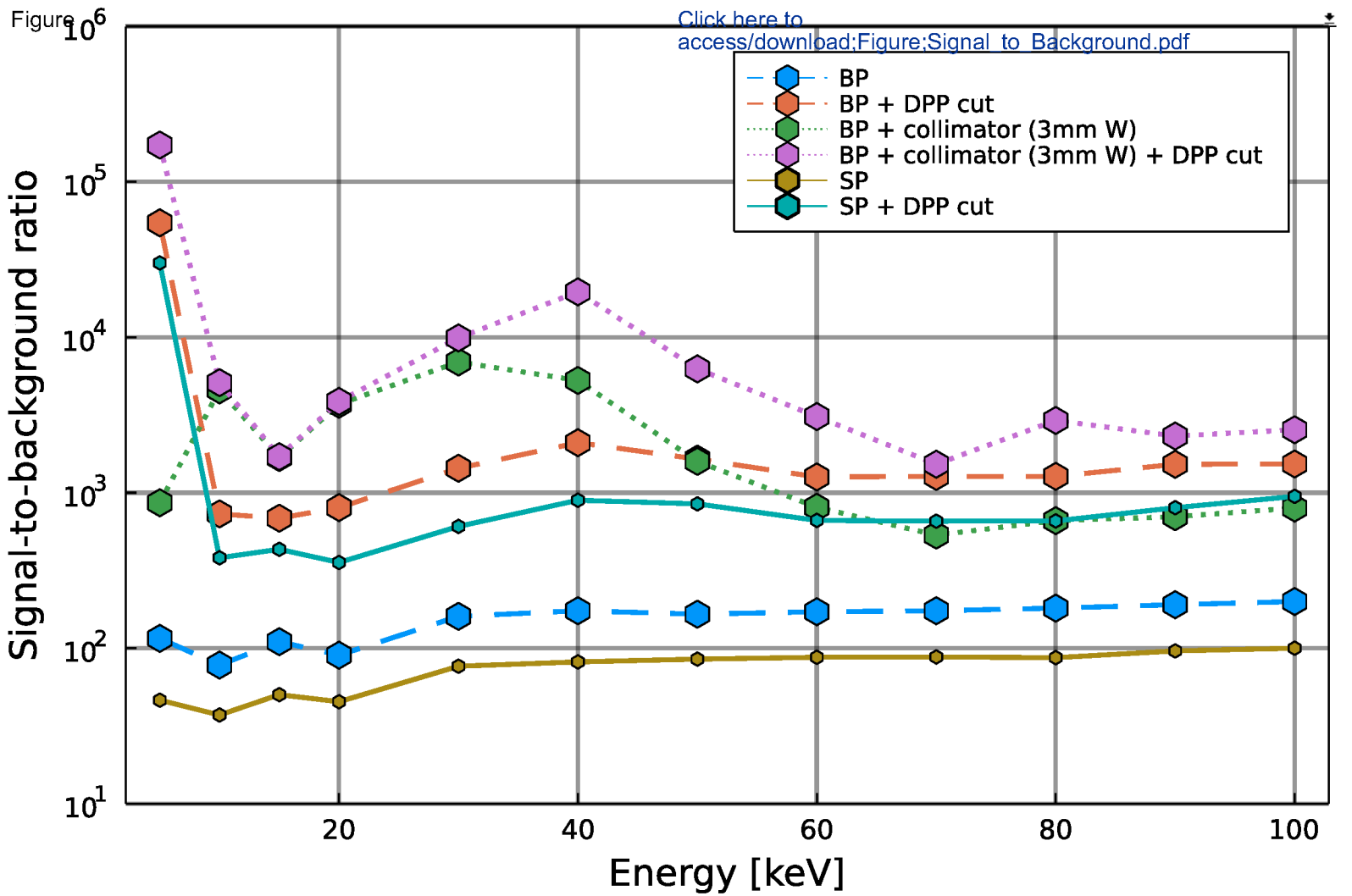






Figure

[Click here to access/download;Figure;Background_level.pdf](#)



Development of Multi-element Monolithic Germanium Detectors for X-ray Detection at Synchrotron Facilities

L. Manzanillas^{a,*}, S. Aplin^b, A. Balerna^c, P. Bell^d, J. Casas^e, M. Cascella^d, S. Chatterji^f, C. Cohen^g, G. Dennis^f, P. Fajardo^g, H. Graafsma^h, H. Hirsemann^h, F. J. Iguaz^a, K. Klementiev^d, T. Kołodziejⁱ, T. Martin^g, R. Menk^k, F. Orsini^a, M. Porro^{b,l}, M. Quispe^e, B. Schmitt^j, N. Tartoni^f, M. Turcato^b, C. Ward^d, E. Welter^h

^aSynchrotron SOLEIL, L'Orme des Merisiers, Départementale 128, Saint-Aubin, 91190, France

^bEuropean XFEL, Holzkoppel 4, Schenefeld, 22869, Germany

^cLaboratori Nazionali di Frascati, Via Enrico Fermi 54 (già 40), Frascati (Roma), 00044, Italy

^dMAX IV Laboratory, Lund University, Fotongatan 2, Lund, 224 84, Sweden

^eALBA-CELLS Synchrotron Radiation Facility, Carrer de la Lluna 2-26, Cerdanyola del Valles, Barcelona, 08290, Spain

^fDiamond Light Source Ltd, Harwell Science and Innovation Campus, Didcot, OX1 10DE, United Kingdom

^gThe European Synchrotron Radiation Facility (ESRF), 71 avenue des Martyrs, Grenoble, 38000, France

^hDeutsches Elektronen-Synchrotron DESY, Notkestr. 85, Hamburg, 22607, Germany

ⁱJagiellonian University, ul. Golebia 24, Kraków, 31-007, Poland

^jPaul Scherrer Institute, Forschungsstr 111, Villigen PSI, 5232, Switzerland

^kElettra-Sincrotrone Trieste, S.C.p.A., S.S. 14-km 163.5 in AREA Science Park, Basovizza, Trieste, 34149, Italy

^lDepartment of Molecular Sciences and Nanosystems, Ca' Foscari University of Venice, Dorsoduro 3246, Venezia, 30172, Italy

Abstract

In past years efforts have concentrated to the developments of arrays of Silicon Drift Detectors for X-ray spectroscopy. This is in stark contrast to the little effort that has been devoted to the improvement of germanium detectors, in particular for synchrotron applications. Germanium detectors enable to detect with better energy resolution and more efficiently photons of considerable higher energy with respect to silicon detectors. In this context, the detector consortium of the European project LEAPS-INNOV has set an ambitious R&D program devoted to the development of a new generation of multi-element monolithic germanium detectors for X-ray detection. In order to improve the performance of the detector under development, physics simulations of the different detector design options have been performed. In this contribution, the efforts in terms of R&D are outlined with focus on the modelization of the detector geometry and first performance results.

Keywords: Germanium detectors, Semiconductors, Synchrotrons

1. Introduction

2 X-rays Absorption Fine Structure (XAFS) has been widely used in experiments at syn-
3 chrotron facilities in order to determine the electronic and geometrical structure of a sample.

*Corresponding author

Email address: luis.manzanillas@synchrotron-soleil.fr (L. Manzanillas)

Preprint submitted to Nuclear Physics A

September 6, 2022

4 XAFS and similar techniques require energy resolving photon-counting detectors capable to cope
5 with a high count rate. The ongoing XAFS experiments at synchrotron facilities are limited by
6 the performance of the current generation of Silicon (Si) and Germanium (Ge) detectors [1].
7 While efforts have concentrated to the development of arrays of Silicon Drift Detectors (SDDs),
8 little effort has been devoted to the improvement of Hyper-Pure Germanium (HPGe) detectors.
9 HPGe detectors provide better energy resolution and detection efficiency for photons of consid-
10 erable higher energy with respect to SDDs. The detector consortium of the European project
11 LEAPS-INNOV [2, 3] has set an ambitious R&D program devoted to the development of a new
12 generation of multi-element monolithic HPGe detectors for X-ray detection. This new genera-
13 tion of HPGe detectors will be able to cope with a high throughput in a broad energy range, from
14 5 to 100 keV. Accepting and processing a high count rate without degradation of the energy res-
15 olution are crucial for the success of this new new generation of HPGe detectors. Therefore, new
16 electronics are being also developed as part of the project. This new electronics will be able to
17 process count rates ranging from 20 kcps/mm² up to 250 kcps/mm², keeping an excellent energy
18 resolution and minimizing dead time.

19 HPGe detectors are built as single contact or segmented detectors. While in single contact
20 detectors the noise decreases because there is no capacitance coupling with other neighboring
21 contacts, it limits the count rate that the detector can accept without pile-up. In contrast, in seg-
22 mented HPGe detectors a considerable increase of count rate keeping a tolerable pile-up proba-
23 bility can be achieved. The strategy of the project is to develop HPGe segmented detectors. A
24 sketch of a HPGe segmented detector being developed is shown in Figure 1. The segmentation
25 of the readout contacts consists of a central hexagonal shape surrounded by six trapezoids and
26 three outer segments. Moreover, a guard ring surrounds the readout contacts.

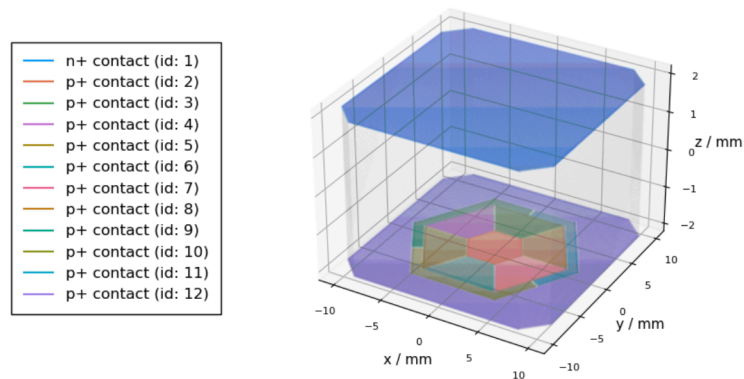


Figure 1: Geometry of HPGe detector prototype being developed by the LEAPS-INNOV detector consortium. The detector dice dimensions are 21×21×4 mm³. The top of the detector (n+) facing the X-rays is non segmented and it is used to place the high voltage connection. The bottom of the detector (p+) is segmented and it is used to readout the signals in hole collection mode.

27 The detectors under development will be fabricated from crystals with dice geometry and
28 dimensions of 21×21×4 mm³ as shown in Figure 1. The area of each read out electrode shown
29 in Figure 1 will be around 20 mm² and corresponds to a big pixel (BP) configuration. A similar
30 segmentation with a contact area of around 5 mm² corresponds to a small pixel (SP) configura-
31 tion. The detectors will be made of n-type germanium crystals, with an expected net impurity

32 concentration of the order of $\sim 10^{10} / \text{cm}^3$.

33 Aiming to study, characterize and optimize the performance of the HPGe detectors under de-
34 velopment, detailed multi-physics simulations were performed and are described in next section.

35 2. Simulation chain

36 In most of XAFS experiments, only the energies deposited in the detectors are recorded.
37 However, the time development of the charges induced in the read out electrodes i.e. the pulses,
38 are used to optimize the acquisition parameters to maximize the detector performance. In ad-
39 dition, pulse shape analysis can be used to improve the position reconstruction and background
40 rejection efficiency. In particular, the rejection of events with energy deposition being detected
41 in several electrodes, i.e. multi-site events, is vital to decrease the background and to improve
42 the energy resolution.

43 A precise simulation of the detector pulses is essential to develop and optimize the required
44 algorithms for signal selection and energy reconstruction. To this end, a complete simulation
45 chain, including all the steps from the interaction of X-rays with the HPGe detector and its
46 environment to a reconstructed energy spectrum using simulated data-like raw waveforms was
47 developed. Figure 2 shows the flowchart of the simulation chain. The required information about
48 the HPGe detector such as the detector geometry, impurity density, bias voltage, among others,
49 are used to calculate the detector fields. Once all the information about the fields has been com-
50 pleted, the information about the interaction of the X-rays with the detector is used to simulate
51 perfect pulses. The interaction of the X-rays with the HPGe detector and its environment is per-
52 formed using the Geant4 simulation toolkit [4]. Finally, the signal amplification and electronics
noise are included and a data-like waveform is produced for each event.

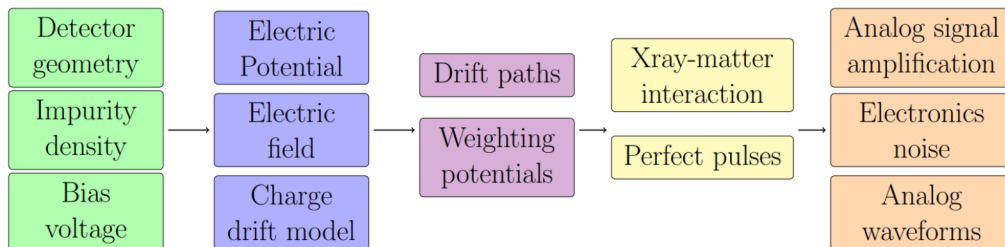


Figure 2: Flowchart of the simulation chain.

53

54 2.1. Simulation of detector fields

55 The shape of the pulses of the signals in HPGe detectors is mainly governed by the fields in
56 the detector. These fields are dependent on the detector and electrodes geometry, bias voltage and
57 impurity profile. To simulate the detector fields, a bias voltage of 200 V and an impurity density
58 of the order of $10^{10} / \text{cm}^3$ (\sim constant) in the bulk material was used. A precise calculation
59 of all the detector fields is crucial to a faithful reproduction of the detector signals. To this
60 end, the SolidStateDetectors.jl (SSD) [5] and COMSOL-Multiphysics [6] packages were used to
61 calculate the detector fields. These packages allow one to calculate the electric potential, electric
62 field and weighting potentials in the whole detector volume. In addition, SSD also allows one
63 to simulate the drifts of charge carriers in solid state detectors together with the corresponding

64 pulses. Moreover, SSD has been optimized for large HPGe detectors, and has been developed as
 65 an open software package using the **julia** programming language [7] to facilitate the integration
 66 of additional developments. Thus, the full simulation chain was developed using SSD and **julia**.
 67 To compute the electric potential and the electric field, Poisson's equation must be solved

$$\nabla(\epsilon_r(\vec{r})\nabla\Phi(\vec{r})) = -\frac{\rho(\vec{r})}{\epsilon_0} \quad (1)$$

68 with $\Phi(\vec{r})$ being the electric potential, ρ the charge density, ϵ_r the dielectric distribution, and
 69 ϵ_0 the dielectric constant of the vacuum. In SSD, the electric potential is calculated through
 70 the successive over relaxation (SOR) method. Equation 1 is numerically solved on a three-
 71 dimensional adaptive grid. The adaptive grid allows for multithreading and saves computation
 72 time since it only increases the grid point density in areas where it is critical. The electric field is
 73 calculated from the electric potential $\Phi(\vec{r})$. The field vector components on each grid point are
 74 the means of the electric field in each direction calculated as finite differences.

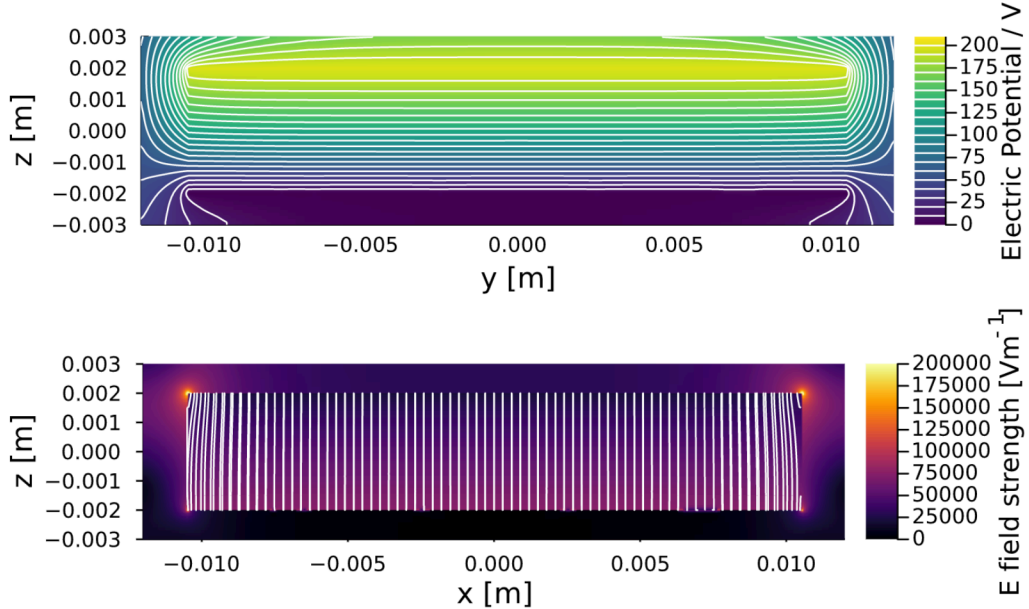


Figure 3: Top: Electric potential in the HPGe detector with big pixel geometry configuration, calculated with the SSD package and assuming a bias voltage of 200 V. Bottom: Electric field strength and electric field lines.

75 Figure 3 shows the electric potential (Top) and the electric field lines (Bottom) that have been
 76 calculated with SSD assuming a bias voltage of 200 V. The Ge sensor is fully depleted, and in
 77 almost the whole detector the charge carriers will drift vertically in direction of the electrodes.

78 2.2. Simulation of detector pulses

79 In HPGe detectors the electric signals corresponds to the sum of the charges induced in the
 80 electrodes of the detector by all the drifting electrons and holes. In SSD, the Shockley-Ramo
 81 theorem is used to calculate the time development of the induced charge in each electrode. The

82 charges carries will be seen and collected by a given electrode as a function of its position and
 83 the weighting potential of the electrode. The weighting potential is a theoretical potential that
 84 describes what fraction of a charge at position \vec{r} is seen by a contact C_i . The weighting potential
 85 can take values between 0, i.e. the charge is not seen by the electrode, and 1, i.e. the charge
 86 is seen and collected by the electrode. The weighting potential is calculated solving Laplace
 87 equation

$$\nabla(\epsilon_r(\vec{r})\nabla\Phi_i^w(\vec{r})) = 0 \quad (2)$$

88 where $\Phi_i^w(\vec{r})$ is the electric potential and $\epsilon_r(\vec{r})$ is the dielectric distribution. To calculate the
 89 weighting potential of a given contact, a voltage of 1 V is applied to that contact and 0 V to all
 90 other contacts. Figure 4 shows the calculated weighting potential for the central contact with
 91 hexagonal shape of the BP detector geometry configuration.

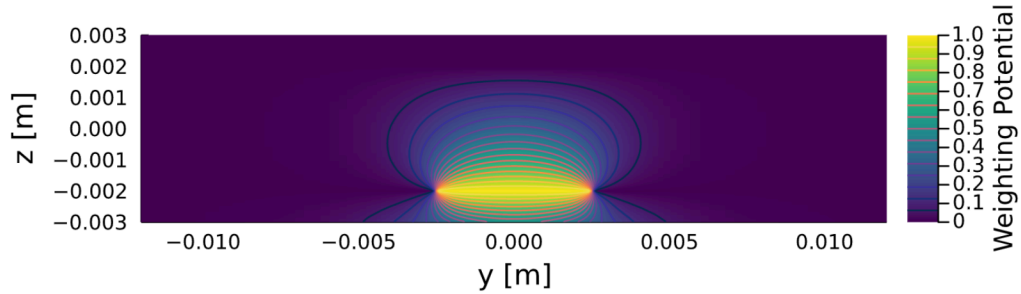


Figure 4: Weighting potential of the hexagonal shape central electrode of the BP geometry configuration.

92 The drift velocity vectors are calculated separately for electrons and holes for each grid point
 93 using the calculated electric field and the respective electron or hole drift velocity model. The de-
 94 fault drift velocity model implemented in SSD uses measured parameters for HPGc at 77 K [8].
 95 Using these parameters the charge carriers are drifted and noiseless pulses are generated in each
 96 readout contact. The final steps in the simulation of the pulses include the signal amplification
 97 and electronics noise. The former is accounted for by convoluting the perfect pulses with a simu-
 98 lated transfer function. The electronics noise is included adding baseline data from a commercial
 99 HPGc detector to the amplified pulses. These preliminary transfer function and electronics noise
 100 will be adjusted with the final measured parameters once the detectors are available.

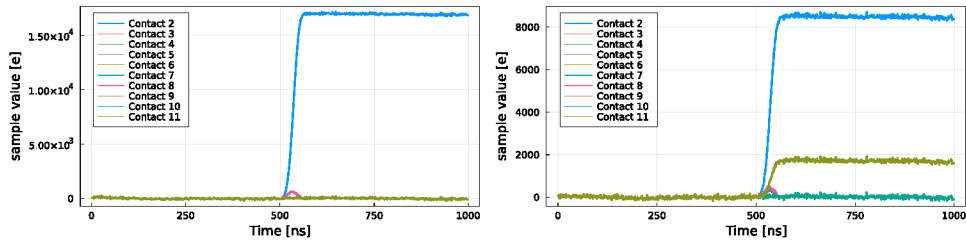


Figure 5: Left: Example of simulated waveforms for an event collected in a single contact. Right: Example of simulated waveforms for an event showing charge sharing being collected in two contacts. The small "bump" without net transfer of charge observed in neighboring channels is the result of the mutual capacitance coupling between contacts.

101 Figure 5 shows simulated waveforms containing pulses with all the steps of the simulation
 102 chain for an event collected in a single contact (Left) and a charge sharing event collected in two
 103 contacts (Right). A small bump is also induced in the neighboring contacts without net transfer
 104 of charge. This "bump" induced in neighboring channels is the result of the mutual capacitance
 105 coupling between neighboring contacts. A total capacitance for each contact of around 1 pF and
 106 3 pF was estimated with SSD for the SP and BP configurations respectively.

107 3. Detector performance

108 To estimate the detector performance, an incident X-ray beam is sent in the detector with
 109 energies ranging from 5 keV to 100 keV. For each energy, about 2 M of events were simulated.
 110 For every event the complete simulation chain was applied and the corresponding data-like raw
 111 waveforms of all readout contacts were generated. The energy of each event was estimated
 112 by applying a trapezoidal filter to the data-like raw waveform of the contact with the highest
 113 collected charge. This trapezoidal filter is expected to be implemented in the DPP. The final
 114 energy spectrum obtained in this way with all the reconstructed events was used to define a region
 115 of interest (RoI) and a background region (BR). The RoI was defined with a band around the
 116 energy of the beam ($E \pm 0.5$ keV), while the background region was taken from an equivalent band
 117 with the same width shifted 3.5 keV to lower energies. The signal efficiency and background
 118 level were defined as the number of events in the RoI or BR over the total number of events in
 119 the spectrum. The potential of using a Digital Pulse Processor (DPP) capable of performing an
 120 online selection of the events was also studied. Thus, this DPP selection consisted in identifying
 121 and removing charge sharing events using an energy threshold of 1 keV. Charge sharing events
 122 deteriorate the energy resolution and populate the background region.

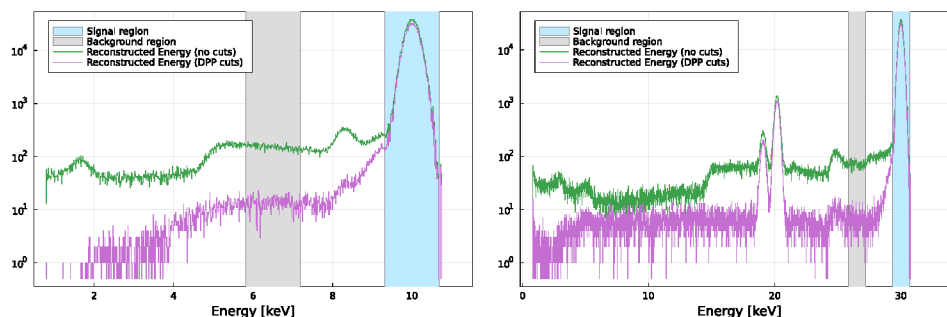


Figure 6: Left: Reconstructed energy spectrum for a direct X-ray beam of 10 keV. Right: Reconstructed energy spectrum for a direct X-ray beam of 30 keV. Two peaks around 20 keV are also observed and have their origin in the escape peaks of the Ge fluorescence.

123 Figure 6 shows two examples of reconstructed energy spectra for a direct X-ray beam of
 124 10 keV and 30 keV with (violet) and without (green) a DPP selection. The RoI and BR are
 125 shown with a blue and with a grey band respectively. The main peaks in the spectra corresponds
 126 to the energy of the beam. Above 10 keV two other peaks are also present as can be seen in
 127 Figure 6 (Right). These two peaks correspond the escape peaks of the Ge fluorescence (9.86
 128 keV, 9.89 keV and 10.98 keV).

129 From the energy spectra shown in Figure 6, the detector performance can be extracted. Thus,
 130 Figure 7 (Left) shows the estimated signal efficiency in the region of interest. The lower values

131 are obtained for the small pixels detector configuration. Values close to 100% are obtained for
 132 energies below 11 keV where most of the photons are completely absorbed by photoelectric effect
 133 and the corresponding electrons are absorbed in a small volume of the detector. A decrease of the
 134 signal efficiency is observed between 11 keV and 20 keV because of the Ge fluorescence.
 135 The photons from the Ge fluorescence escape the detector, decreasing the number of events in
 136 the main peak.

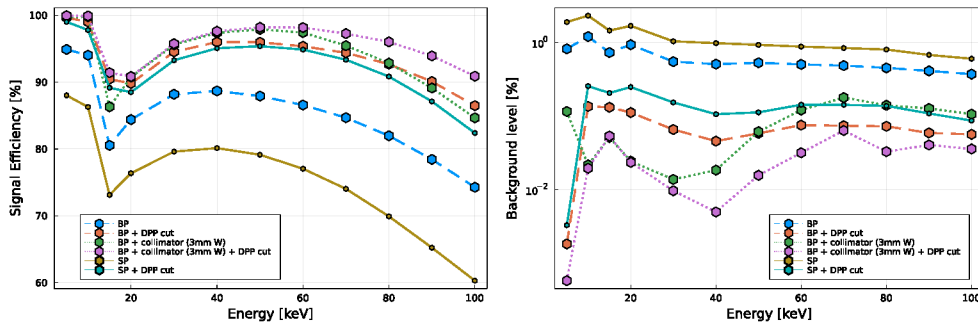


Figure 7: Left: Estimated signal efficiency for the SP and BP configuration with and without a DPP selection, and BP plus a collimator with and without a DPP selection. Right: Estimated background level using the same configuration as the left plot.

137 The simulations also showed that the efficiency can be improved by using either a collimator,
 138 or a specific selection with a Digital Pulse Processor (DPP), or both to remove charge sharing
 139 events. In this simulation, the collimator consists in a block of tungsten, with a thickness of 3 mm
 140 covering the whole surface of the HPGe detector and containing holes corresponding to the pixel
 141 geometry. By using a collimator, the inter-pixel regions where most of the charge sharing events
 142 take place are shielded. Given the small pixel area of the small pixel (SP) configuration, the
 collimator was considered only for the BP configuration.

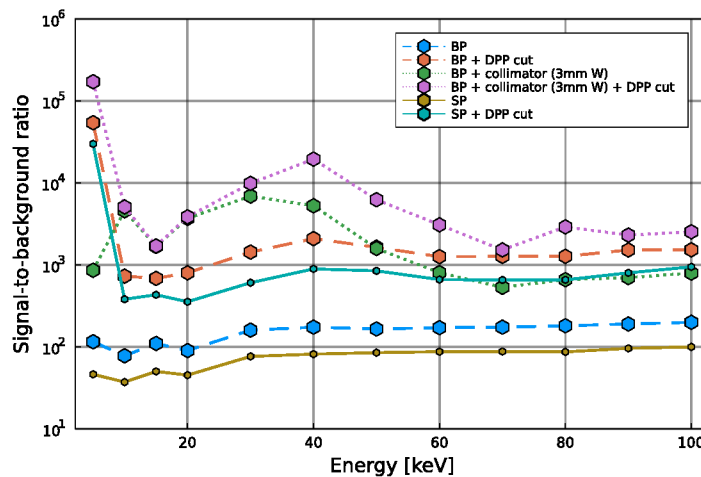


Figure 8: Signal to background ratio in the region of interest for all the configurations studied.

144 Figure 7 (Right) shows the estimated background level. The lowest background level is
145 achieved for the BP configuration in conjunction with a collimator plus a specific DPP selection.
146 This combination allows one to remove most of the events populating the background region.
147 Finally, to evaluate the combined effect of signal efficiency and background level, a signal-to-
148 background ratio parameter was defined. This parameter was evaluated as the coefficient between
149 the signal efficiency and the background level. Figure 8 shows the expected signal-to-background
150 (S/B) ratio for the different configurations under investigation. The target of the project is to
151 achieve a S/B ratio larger than 1000 for energies below 10 keV. From the different configurations
152 analyzed, the best performance is obtained for the BP configuration combining a 3 mm tungsten
153 collimator and a DPP selection, in which a S/B ratio larger than 1000 in the whole energy range
154 is reached.

155 4. Conclusions

156 The LEAPS-INNOV detector consortium has set an ambitious R&D program launched in
157 April 2021 for the development of a new generation of monolithic pixelized HPGe detectors
158 for synchrotron applications. A full simulation chain based on the SSD package and **Julia**^{*} has
159 been developed to study and optimize the performance of the detectors under development. First
160 results suggest that both, signal efficiency and background level, can be highly improved in the
161 region of interest for X-rays with energies ranging from 5 keV to 100 keV, compatible with the
162 requirements. These results translate into an excellent signal-to-background ratio in the whole
163 energy range. The best performance could be obtained combining a specific selection with a
164 DPP and a collimator in order to remove charge sharing events. The simulation chain optimized
165 once the detectors are available for data taking.

166 5. Acknowledgments

167 This project has received funding from the European Union's Horizon 2020 research and
168 innovation programme under grant agreement No 101004728.

169 References

- 170 [1] N. Tartoni, et al., "Hexagonal Pad Multichannel Ge X-Ray Spectroscopy Detector Demonstrator: Comprehensive
171 Characterization," in *IEEE Transactions on Nuclear Science*, vol. 67, no. 8, pp. 1952-1961, Aug. 2020.
- 172 [2] LEAPS pilot to foster open innovation for accelerator-based light sources in Europe, European Union's Horizon
173 2020, Grant Agreement No 101004728.
- 174 [3] F. Orsini, et al., "XAFS-DET: a new high throughout X-ray spectroscopy detector system developed for synchrotron
175 applications", August 2022 NDIP2020 Conference, this record.
- 176 [4] S. Agostinelli *et al.* [GEANT4], "GEANT4—a simulation toolkit," *Nucl. Instrum. Meth. A* **506** (2003), 250-303
177 doi:10.1016/S0168-9002(03)01368-8
- 178 [5] I. Abt, et al., "Simulation of semiconductor detectors in 3D with SolidStateDetectors.jl," *JINST* **16** (2021) no.08,
179 P08007 doi:10.1088/1748-0221/16/08/P08007 [arXiv:2104.00109].
- 180 [6] COMSOL Multiphysics® v.6.0. www.comsol.com. COMSOL AB, Stockholm, Sweden.
- 181 [7] Bezanson, J. et al., 2012. Julia: A fast dynamic language for technical computing. [arXiv:1209.5145].
- 182 [8] B. Bruyneel, P. Reiter and G. Pascovici, "Characterization of large volume HPGe detectors. Part I: Electron and
183 hole mobility parameterization," *Nuclear Instruments and Methods in Physics Research Section A: Accelerators,*
184 *Spectrometers, Detectors and Associated Equipment.* Volume 569, Issue 3, 21 December 2006.

Dear Referees and Editor,

Please find in the attached files our manuscript in which we have summarized the poster entitled "Development of Multi-element Monolithic Germanium Detectors for X-ray Detection at Synchrotron Facilities" that was presented at the NDIP20 conference in Troyes.

The article presents the ongoing simulation efforts in order to optimize the performance of the new generation of hyper-pure germanium detectors (HPGe) under development. In particular, we present the details of the simulation chain that we have developed for this purpose. Moreover, first performance results are also presented.

If you have any comments do not hesitate to let us know.

Thanks in advance

Luis Manzanillas on behalf of the LEAPS-INNOV detector consortium.